

05,13

## Formation of waveguiding channels for spin waves in a laser-induced magnonic microwaveguide

© I.O. Filchenkov, A.A. Grachev, A.V. Sadovnikov

Saratov National Research State University,  
Saratov, Russia

E-mail: infachforever@gmail.com

Received December 4, 2024

Revised January 21, 2025

Accepted January 29, 2025

In this study, a method of directional spin wave branching in a rectangular waveguide made of yttrium iron garnet induced by laser radiation is demonstrated using numerical studies. It is demonstrated that the central part of the waveguide is heated by the laser beam along its entire length, leading to the emergence of a saturation magnetization gradient in the affected region. The application of laser radiation effectively „divides“ the waveguide into two independent narrow waveguide channels for spin waves, thereby enabling the observation of the phenomenon of spatial pumping of spin waves. This technique enables the modulation of spin wave propagation by directing them into either half of the waveguide, thereby establishing a tap of the spin-wave signal. This approach opens new possibilities for dynamically controlling magnon devices with high accuracy and speed, and enables the development of new types of logic elements and switches for magnon circuits.

**Keywords:** magnonics, dipolar interaction, laser heating, coupled structures.

DOI: 10.61011/PSS.2025.03.60876.331

### 1. Introduction

Spin waves are collective oscillations of magnetic spin moments in ferromagnetic materials and are a fundamental object of study in magnonics — a fast-developing field of science, aimed at use of such waves for transmission and processing of information. Spin waves may spread in the frequency range from several GHz to 10 THz, which makes them attractive for use in microwave electronics and telecommunications. Wavelengths in these systems may vary from several nanometers to microns, depending on the material and frequency of excitation, which makes it possible to develop the devices at micro- and nanoscales [1–3].

One of the key advantages of spin waves is their low level of energy losses in propagation compared to electric signals in semiconductor materials. In contrast to conventional electronics, based on movement of charged particles (electrons), in magnonics information is transmitted via oscillations of spin moments — magnons, which minimizes effects related to Joule heating and ohmic losses. This opens prospects for development of energy-efficient devices with high speed of information processing, which makes magnonic systems competitive in respect to the state-of-the-art semiconductor solutions [4,5].

Among different materials applied in magnonics, yttrium-iron garnet (YIG) stands apart as one of the most promising. YIG has one of the lowest values of spin-wave attenuation among the known materials, which makes it ideal for development of waveguide structures and other magnonic devices [6]. Due to low losses and high Q factor, YIG is the basis for development of miniature waveguide structures, which may be scaled to micron and nanometer dimensions.

This opens the possibility to create compact and energy-efficient devices for processing of information signals, such as filters, demultiplexers etc. [7–9].

To develop multifunctional magnon devices, it is important to not only excite spin waves, but be able to control their propagation. Several methods exist to control spin waves, which may be used to change their frequency, amplitude or direction of propagation, for example, addition of ferromagnetic resonant cavities to waveguide structures [10] or addition of geometric irregularities to the waveguide structure [11]. This opens new opportunities for development of complicated magnonic circuits and logical elements.

The method to control spin waves is of special interest, where local irregularities are developed, which lead to appearance of the areas with heterogeneous distribution of the internal magnetic field. For example, one of such methods is the use of piezoelectric layers applied above the YIG film [12,13]. When voltage is applied on the piezoelectric layer, mechanical deformation occurs, which is transmitted to the YIG film by changing the internal magnetic field therein. This results in the change of the spectrum of spin waves and makes it possible to flexibly control their characteristics.

The method of saturation gradient development by laser heating warrants special attention [14,15]. This approach is based on changing the magnetic properties of the material when exposed to heat, which makes it possible to locally control magnetization of saturation and, accordingly, behavior of spin waves. In case of YIG, which is characterized by high temperature dependence of magnetization, the laser

impact may considerably change the characteristics of spin waves propagation.

In this paper the method of numerical studies shows the way to couple spin waves in a rectangular waveguide from YIG, under the impact of the laser radiation on the waveguide surface. Along the entire length of the waveguide, the laser beam heats the central part, which causes drastic decrease of saturation magnetization in the area of exposure. As a result the waveguide „is split“ into two independent narrow waveguides, since spin waves must overcome the area with lower magnetization. Such method makes it possible to control distribution of spin waves, directing them to one or other half of the waveguide and, therefore, creating the spin signal coupler controlled by laser radiation. The considered method opens new opportunities for dynamic control of magnonic devices with high precision and speed, and also makes it possible to develop new types of logical elements and switches for magnonic circuits.

## 2. Studied structure description

The scheme of the studied structure is shown in Figure 1. The considered structure is a microwaveguide from YIG film, with width of  $w = 440 \mu\text{m}$ , thickness of  $t = 10 \mu\text{m}$ , and structure length was 8 mm. Film saturation magnetization was  $4\pi M_0 = 1750 \text{ G}$ . The film is on the substrate from gadolinium-gallium garnet (GGG) with thickness of  $500 \mu\text{m}$ . Using laser heating, a rectangular area is formed along the entire length of the waveguide, which „separates“ the waveguide into 2 waveguide channels (Figure 1): channel 1 ( $S_1$ ) and channel 2 ( $S_2$ ). Width of the laser heating area is specified as  $d$ . On one side of the waveguide there is an exciting microstrip antenna  $P_{in}$ , at the same time the antenna occupies a half of the microwaveguide width and is in channel 1. The receiving microstrip antennas are on the other side of microwaveguide and are specified as  $P_{out1}$  and  $P_{out2}$ . Output antennas occupy half of the waveguide width and are located in channel 1 and in channel 2, respectively. Input and output antennas have width of  $30 \mu\text{m}$  and length of  $220 \mu\text{m}$ . The structure was placed in the external static magnetic field  $H_0 = 1300 \text{ Oe}$ , oriented along the axis  $y$  to effectively excite a surface magnetostatic wave (SMW).

## 3. Micromagnetic modeling

To study the dynamics of magnetization under exposure of laser heating, a method of micromagnet modeling was used, made in a software suite mumax<sup>3</sup> [16] and based on a solution to Landau–Lifshitz–Helmholtz equation (LLH) by method of Dormand-Prince:

$$\frac{\partial \mathbf{M}}{\partial t} = \gamma [\mathbf{H}_{\text{eff}} \times \mathbf{M}] + \frac{\alpha}{M_0} \left[ \mathbf{M} \times \frac{\partial \mathbf{M}}{\partial t} \right], \quad (1.1)$$

where  $\mathbf{M}$  is magnetization vector,  $\alpha = 10^{-5}$  is attenuation parameter,  $\mathbf{H}_{\text{eff}} = \mathbf{H}_0 + \mathbf{H}_{\text{demag}} + \mathbf{H}_{\text{ex}} + \mathbf{H}_a$  is effective mag-

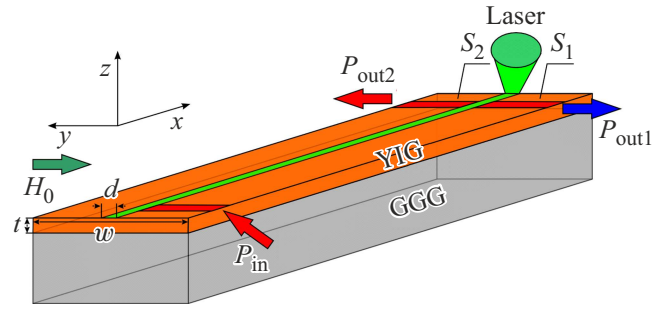


Figure 1. Scheme of the studied magnonic structure.

netic field,  $\mathbf{H}_0$  — external magnetic field,  $\mathbf{H}_{\text{demag}}$  is demagnetization field,  $\mathbf{H}_{\text{ex}}$  is exchange field,  $\mathbf{H}_a$  is anisotropy field,  $\gamma = 2.8 \text{ MHz/Oe}$  is gyromagnetic ratio in YIG film.

To decrease the reflection of the signal from the boundaries of the estimated area ( $x = 0$  and  $x = 8 \text{ mm}$ ) the calculation included areas ( $0 < x < 0.5 \text{ mm}$  and  $7.5 < x < 8 \text{ mm}$ ) in the form of absorbing layers (Perfectly Matched Layers) with increased values of the coefficient  $\alpha$  (up to  $\alpha = 1$ ). The exchange constant in YIG film is  $A_{\text{ex}} = 3.612 \text{ pJ/m}$ . The size of one grid cell was  $5 \times 3 \times 2 \mu\text{m}$ , to avoid the impact of heterogeneous exchange. At the same time, the calculation with the decreased size of the cell does not provide substantial changes in the produced static and dynamic characteristics. This is explained by the fact that within this task we do not take into account the exchange waves (exchange length  $\sim 20 \text{ nm}$ ), and the least wavelength of SMW is  $10 \mu\text{m}$ .

To account for impact of local laser heating at temperature  $T$ , the modeling included the area with the decreased magnetization of saturation  $M_{0r}$ . In this case the assumption on the linear dependence of saturation magnetization decrease with growth of value  $T$ , since the temperature variation temperature range exceeded value  $T_{\text{RT}} + 8^\circ\text{C}$ , which is considerably lower than Curie temperature  $T_{\text{K}} = 285.85^\circ\text{C}$  for YIG, where  $T_{\text{RT}} = 27^\circ\text{C}$  — room temperature. Therefore, temperature variation causes a change in saturation magnetization in accordance with the linear dependence of magnetization on temperature [17,18]:

$$M_{0r}(x, y) \approx M_0 - \beta[T(x, y) - T_m],$$

where  $\beta = 313 \text{ A K}^{-1} \text{ m}^{-1}$ . Since the microwaveguide is formed from a rather thin YIG film ( $t = 10 \mu\text{m}$ ), the heating along the thickness was deemed homogeneous. The laser heating area width in the calculation varied from 30 to  $50 \mu\text{m}$ . Besides, the area with the varied saturation magnetization was taken as distribution of Gaussian beam along the width, which makes it possible to model the situation of heterogeneous distribution in space.

To excite propagating spin waves, the input signal was specified in the form of  $h_z(t) = h_0 \cdot \sin c(2\pi f_c t)$  with central frequency  $f_c = 7 \text{ GHz}$ ,  $h_0 = 0.1 \text{ Oe}$ . Then the value of dynamic magnetization  $m_z(x, y, t)$  in the output regions

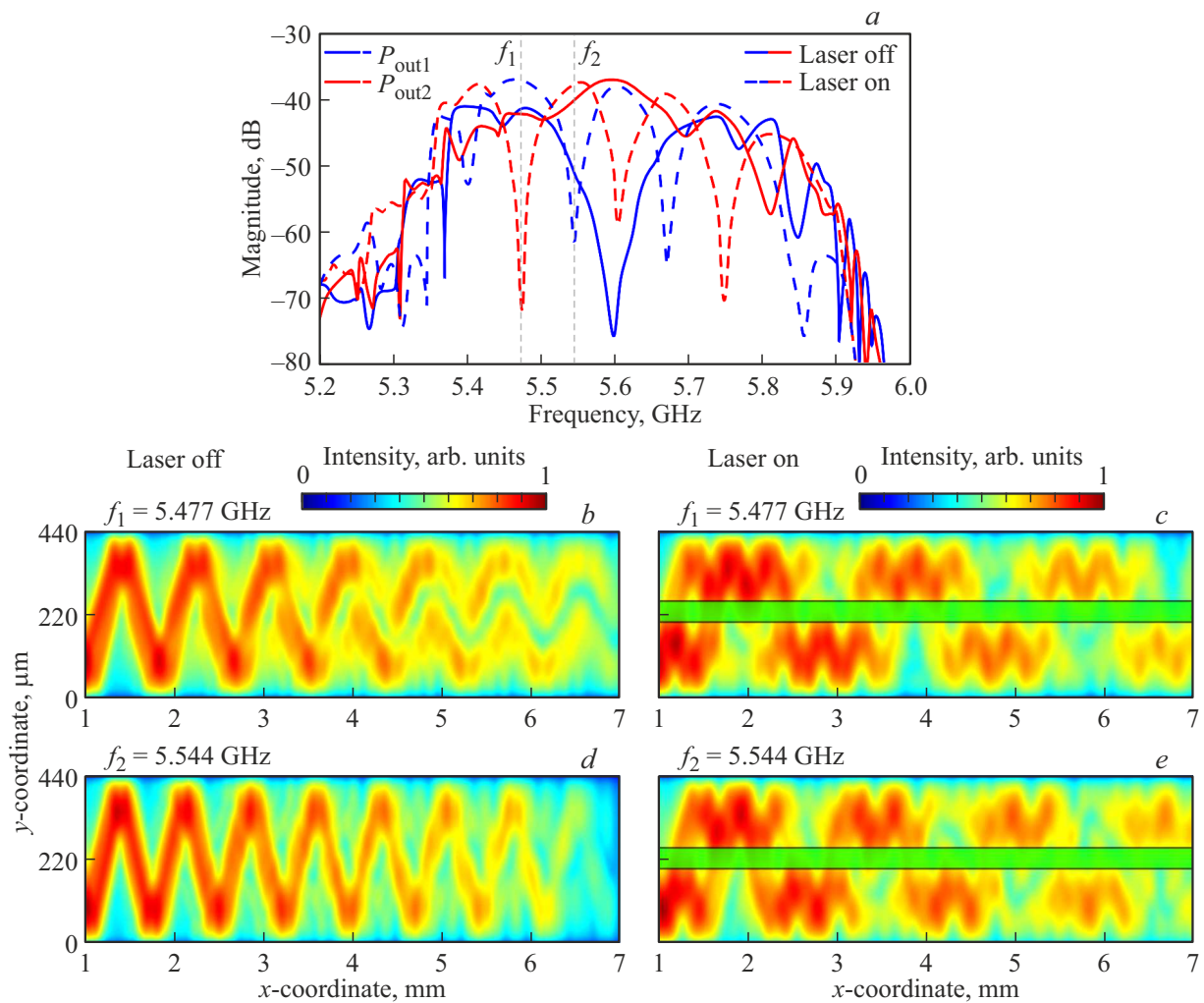


**Figure 2.** *a* — amplitude-frequency characteristics of the studied structure in absence of laser heating (solid curves) and in presence of laser heating (dashed curves) at different output ports (blue —  $P_{out1}$ , red —  $P_{out2}$ ); *b, d* — spatial maps of spin wave distribution in absence of laser heating and *c, e* — in presence of laser heating.

$P_{out1,2}$  was recorded with a step of  $\Delta t = 75$  fs for 500 ns. As a result, it was possible to plot the frequency dependence of the dynamic magnetization of the output regions  $P_{out1,2}$  using the Fourier transform. At the same time the output dynamic magnetization was averaged by size of output antennas.

To analyze behavior of spin waves in the studied structure, numerical calculations were completed for the amplitude-frequency response (AFR) of spin-wave signals (Figure 2, *a*), obtained at output antennas  $P_{out1}$  and  $P_{out2}$ . Two modes were considered: without laser heating (solid blue line for  $P_{out1}$ , solid red line for  $P_{out2}$ ) and with laser heating, generating local heterogeneity of magnetization (dashed blue curve for  $P_{out1}$ , dashed red curve for  $P_{out2}$ ).

In absence of laser heating, the spin wave excited by an input microstrip antenna  $P_{in}$ , propagates in the structure, occupying its full width. Since the antenna excites a wave only at half of the waveguide width, the initial propagation of the wave goes from one edge of the waveguide along

the diagonal line to the opposite edge, with subsequent multiple reflections. You may say that excitation of a spin wave for the case when there is no laser heating causes a „zigzag-shaped“ spread of SMW along the entire length of the waveguide. This type of excitation provides for the availability of the area of spin-wave signal non-passage in the area of the antenna  $P_{out1}$  at frequency  $\sim 5.6$  GHz. Besides, the area of signal non-passage for the antenna  $P_{out2}$  is absent in the spectrum of spin waves. This is related to asymmetric excitation of the wave, since the input antenna is located only at the half of the waveguide width.

When exposed to the laser heating, an area is formed along the waveguide length with gradient distribution of saturation magnetization with width of  $d = 30 \mu\text{m}$ , which in turn causes the waveguide separation into two parallel-oriented waveguide channels. This results in transformation of spin-wave distribution in the considered system.

Exposure of the YIG microwaveguide surface to laser heating causes formation of specific power dips in AFR

recorded at the outputs  $P_{\text{out1}}$  and  $P_{\text{out2}}$  (Figure 2, *a*, broken lines). The spectrum becomes discreet instead of continuous, which is related to the system transition to the mode of energy pumping between the waveguide channels.

You can see on the maps of spatial distribution of spin wave intensity that with laser heating on (Figure 2, *c* and *e*) the power of the spin wave is periodically pumped between channel 1 and channel 2 with a certain spatial period, which is called the pumping length describing the connection of SMWs propagating along the waveguide channels, which is expressed as  $L = 2\pi/|k_S - k_{AS}|$ , where  $k_S$  and  $k_{AS}$  — wave numbers of symmetric and antisymmetric modes, respectively. The pumping length is numerically equal to the distance along axis  $x$ , during which the spin wave will go from one channel to the other and will then come back.

You may note a qualitative analogy between this structure with laser heating and a system of two laterally bonded magnetic microwaveguides with width of  $200\mu\text{m}$ , separated with an air gap  $d$  [19–21]. Development of waveguide channels causes splitting of a dispersion branch of spin waves in an isolated waveguide into symmetric and antisymmetric modes [12]. This manifests itself in modes beat, when the spin wave power periodically goes from one channel to the other [19]. Beats are caused by the differences in the phase velocities of symmetric and antisymmetric modes, resulting in modulation of spin wave intensity along the waveguide length [20]. Beats of symmetric and antisymmetric modes arising from interaction of the channels through a dipole magnetic field cause frequency selection. At certain frequencies the spin wave power is mostly transmitted to one of the channels, and that causes the observed dips in AFR. This phenomenon highlights the possibility to manage the spectral characteristics of the system using laser heating.

As it was noted previously, when laser heating is switched on with the end width of the heated area, which separates the waveguide into two channels, it is important that width  $d$  was not excessively large, since it causes considerable decrease in the connection between the channels, making signal pumping ineffective [14]. However, the width of laser heating  $d$  may be varied to study the effect of this parameter at system characteristics.

Figure 3 shows AFRs taken from outputs  $P_{\text{out1}}$  (Figure 3, *a*) and  $P_{\text{out2}}$  (Figure 3, *b*) at the change of the laser heating width  $d = 30, 40$  and  $50\mu\text{m}$ . Let us consider output  $P_{\text{out1}}$ , and for more clarity note the frequencies ( $f_3, f_4, f_5$  in Figure 3, *a*) in the range from 5.6 to 5.7 GHz, corresponding to the specific non-passage areas for various values  $d$ . You can see that as  $d$  increases, these non-passage areas observed at AFR move to the area of lower frequencies. This phenomenon manifests itself both at AFR for  $P_{\text{out1}}$  and for  $P_{\text{out2}}$ . Such shift is due to the change of the interaction conditions between the spin wave modes in the waveguide channels, where increase of width  $d$  changes the mode structure of the system. Therefore, use of the laser heating method makes it possible to both couple SMW

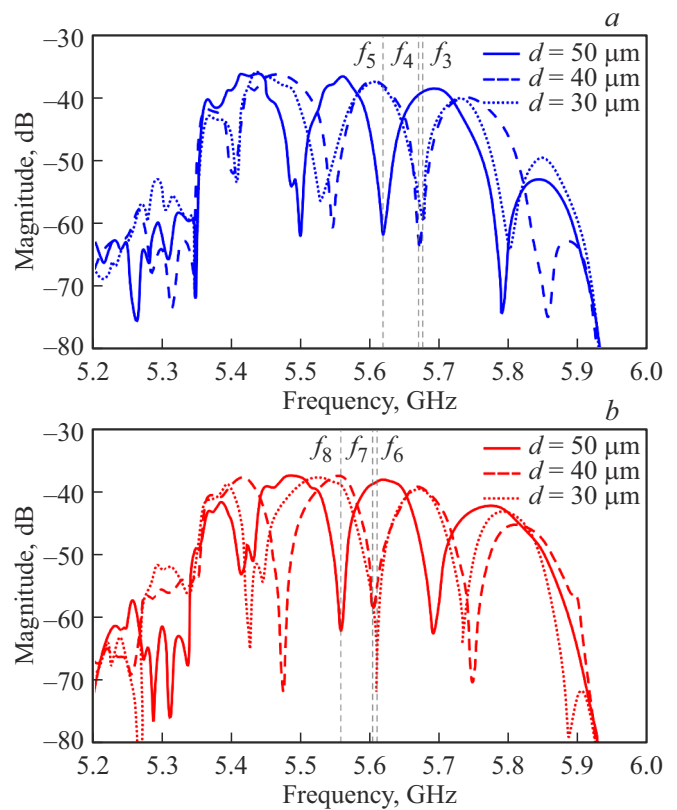


**Figure 3.** AFR in change of laser heating line width  $d = 30\mu\text{m}$  (point curves),  $d = 40\mu\text{m}$  (dashed curves),  $d = 50\mu\text{m}$  (solid curves), taken from outputs: *a* —  $P_{\text{out1}}$ ; *b* —  $P_{\text{out2}}$ .

power and control of the spin wave coupling modes for the spin wave on the output sections of the structure.

## 4. Conclusion

To conclude, it should be noted that the numerical calculations show that the rectangular YIG-waveguide with the area of lower magnetization formed by laser heating makes it possible to successfully create the waveguide channels for spin-wave signal coupling. You may notice a qualitative similarity of the studied effects to the results presented in some papers, where the laterally located waveguides are studied from YIG with a physical gap between them. The advantage of our structure is simplification of geometry due to the fact that the second waveguide is no longer needed — due to use of laser heating, it is possible to form the required waveguide channels. Besides, laser heating also makes it possible to control the signal passage spectrum, not recurring to increase of the input power, change of the external magnetic field or other methods to control spin waves. Such method of spin wave control opens new opportunities for development of devices and technology on the basis of magnetic properties. The studied structure may be used as a Fourier plane filter for microwave signals, providing for selective passage of signals depending on their

frequency and spatial distribution, and may also serve as the basis for development of directed couplers and switches, which makes it promising to implement the devices for processing of information signals in magnonic systems.

### Funding

The study was performed with the support of the Ministry of Education and Science of Russia as part of the Government Task (project No. FSRR-2023-0008).

### Conflict of interest

The authors declare that they have no conflict of interest.

### References

- [1] S.A. Nikitov, D.V. Kalyabin, I.V. Lisenkov, A. Slavin, Yu.N. Barabanenkov, S.A. Osokin, A.V. Sadovnikov, E.N. Beginin, M.A. Morozova, Yu.A. Filimonov, Yu.V. Khivintsev, S.L. Vysotsky, V.K. Sakharov, E.S. Pavlov. *Phys. Usp.* **58**, 10 (2015).
- [2] B. Flebus, S.M. Rezende, D. Grundler, A. Barman. *J. Appl. Phys.* **133**, 16, 160401 (2023).
- [3] B. Flebus, S.M. Rezende, D. Grundler, A. Barman. *J. Phys.: Condens. Matter* **36**, 36, 363501 (2024).
- [4] H. Qin, R.B. Holländer, L. Flajšman, F. Hermann, R. Dreyer, G. Woltersdorf, S. van Dijken. *Nat. Commun.* **12**, 2293 (2021).
- [5] A.A. Serga, A.V. Chumak, B. Hillebrands. *J. Phys. D: Appl. Phys.* **43**, 26, 264002 (2010).
- [6] M. Evelt, V.E. Demidov, V. Bessonov, S.O. Demokritov, J.L. Prieto, M. Muñoz, J.B. Youssef, V.V. Naletov, G. de Loubens, O. Klein, M. Collet, K. Garcia-Hernandez, P. Bortolotti, V. Cros, A. Anane. *Appl. Phys. Lett.* **108**, 17, 172406 (2016).
- [7] S.A. Odintsov, S.E. Sheshukova, S.A. Nikitov, A.V. Sadovnikov. *Phys. Rev. Appl.* **22**, 1, 014042 (2024).
- [8] A. Khitun, K.L. Bao, M. Wang. *J. Phys. D: Appl. Phys.* **43**, 26, 264005 (2010).
- [9] V.E. Demidov, S. Urazhdin, G. De Loubens, O. Klein, V. Cros, A. Anane, S.O. Demokritov. *Phys. Rep.* **673**, 1 (2017).
- [10] A.A. Grachev, E.N. Beginin, A.A. Martyshkin, A.B. Khutieva, I.O. Fil'chenkov, A.V. Sadovnikov. *Izvestiya vuzov. PND* **29**, 2, 254 (2021). (in Russian).
- [11] Y.A. Gubanova, V.A. Gubanov, E.N. Beginin, A.V. Sadovnikov. *J. Exp. Theor. Phys.* **136**, 1, 106 (2023).
- [12] A.A. Grachev, S.E. Sheshukova, S.A. Nikitov, A.V. Sadovnikov. *J. Magn. Magn. Mater.* **515**, 167302 (2020).
- [13] A.V. Sadovnikov, A.A. Grachev, E.N. Beginin, S.E. Sheshukova, Yu.P. Sharaevskii, A.A. Serdobintsev, D.M. Mitin, S.A. Nikitov. *IEEE Trans. Magn.* **53**, 11, 2801604 (2017).
- [14] V.A. Gubanov, V.V. Kruglyak, S.E. Sheshukova, V.D. Bessonov, S.A. Nikitov, A.V. Sadovnikov. *Phys. Rev. B* **107**, 2, 024427 (2023).
- [15] Ia.A. Filatov, P.I. Gerevenkov, M. Wang, A.W. Rushforth, A.M. Kalashnikova, N.E. Khokhlov. *J. Phys.: Conf. Ser.* **1697**, 1, 012193 (2020).
- [16] A. Vansteenkiste, B. Van de Wiele. *J. Magn. Magn. Mater.* **323**, 21, 2585 (2011).
- [17] A. Prabhakar, D.D. Stancil. *Spin Waves: Theory and Applications*. Springer, N.Y. (2009).
- [18] M. Vogel, A. Chumak, E. Waller, T. Langner, V.I. Vasyuchka, B. Hillebrands, G. von Freymann. *Nature Phys.* **11**, 487–491 (2015).
- [19] A.V. Sadovnikov, S.A. Odintsov, E.N. Beginin, S.E. Sheshukova, Yu.P. Sharaevskii, S.A. Nikitov. *Phys. Rev. B* **96**, 14, 144428 (2017).
- [20] A.V. Sadovnikov, E.N. Beginin, S.E. Sheshukova, D.V. Romanenko, Yu.P. Sharaevskii, S.A. Nikitov. *Appl. Phys. Lett.* **107**, 20, 202405 (2015).
- [21] N. Kumar, A. Prabhakar. *IEEE Trans. Magn.* **49**, 3, 1024 (2013).

*Translated by M.Verenikina*